Electrochemistry of Metallofullerene Films: The Major Isomer of Dy@C_{82}

Louzhen Fan, Shangfeng Yang, and Shihe Yang*[a]

Abstract: Solution-cast films of the major isomer of Dy@C_{82} (Dy@C_{82}(I)) have been studied by cyclic voltammetry (CV) in acetonitrile. The films are found to display pronounced and stable redox responses in solution. The reduction/reoxidation processes exhibit large splittings between the first two reduction and reoxidation waves. However, a pair of reversible oxidation and rereduction waves is observed after the reoxidation of a reduced film. The characteristics and the inter-relationship of these waves are uncovered by the CV technique, scanning electron microscopy (SEM), and UV/Vis-NIR spectra. A possible mechanism is proposed for the film electrode processes, which emphasizes the redox-induced structural reorganization of the metallofullerene film by the incorporation and expulsion of electrolyte ions into and out of the film. The influence of the counter ion diffusivity and the ion-pair stability on the electrochemical activity of the metallofullerene film has also been indicated.

Keywords: absorption spectroscopy · electrochemistry · metallofullerenes · thin films

Introduction

Endohedral metallofullerenes have attracted special interest due to the unique properties that are not observed for the empty fullerenes.[1–4] One of the most intriguing properties is the electrochemistry associated with their novel electronic and supramolecular structures.[5–7] In 1993, Suzuki et al. first reported the unusual redox properties of dissolved La@C_{82} which are significantly different from those of empty fullerenes.[8] In organic solution, La@C_{82} exhibits five reversible reduction and one reversible oxidation process, and the six reversible couples appear to be arranged in sets of two, unlike those of empty fullerenes.[9–11] So far many lanthanofullerenes M@C_{82} (M = Y, La, Ce, Pr, Nd, Gd, Tb, Dy, Ho, Er, Lu, etc.) have been electrochemically studied.[12–15] Their electrochemical properties are similar. One common feature is that the difference between the first oxidation and the first reduction potentials is very small due to the open-shell electronic structure. As such, the metallofullerenes are strong electron donors as well as strong electron acceptors compared to empty fullerenes.[8,12–15] It has also been shown that reduction and oxidation of La@C_{82} take place on the carbon cage, leading to a closed-shell electronic structure, so La@C_{82}(−) and La@C_{82}(+) are stable toward air and water.[16] In addition, two isomers have been extracted and isolated for La@C_{82},[17–19] Sc@C_{82},[20] Y@C_{82},[20] and Pr@C_{82}.[21] It was reported that the first oxidation potential of minor isomer shifts negatively by 143 mV relative to that of the major isomer.[19,21]

From the outset, thin films of fullerenes have been the focal point of research. Upon reduction, fullerenes show novel superconducting,[22] magnetic,[23,24] nonlinear optical,[25] and photochemical properties.[26] Therefore, the electrochemical behavior of thin films of C_{60} has been extensively studied,[27–29] and found to be very different from that of the dissolved species. The main feature of the electrochemical properties of the C_{60} film is a large splitting in potential between the reduction and reoxidation waves for the first two electron-transfer reactions, which was interpreted as being due to appreciable reorganization of the film during the reaction. For the metallofullerenes mentioned above, both cationic and anionic charge-transfer complexes could be formed because they are both good electron donors and good electron acceptors. Interesting electric and magnetic properties are expected from such doped charge-transfer metallofullerene solids.[8] However, to our knowledge, electron-transfer reactions of pure metallofullerene films on electrode surfaces have not been reported so far. Most recently, the electrochemistry of La@C_{82} on an artificial lipid film modified electrode has been studied in water,[30] and revealed redox responses analogous to those of the solution phase. It was found that without the artificial lipid film, electron transfer of metallofullerene films on electrodes in aqueous solutions is difficult. We have successfully isolated Dy@C_{82} and its isomers.[31] Here we report the first study on the

[a] Prof. S. Yang, Dr. L. Fan, S. Yang
Department of Chemistry
The Hong Kong University of Science and Technology
Clear Water Bay
Kowloon (Hong Kong)
Fax: (+852) 2358-1594
E-mail: chsyang@ust.hk

  DOI: 10.1002/chem.200304882

electron transfer of a Dy@C_{82}(I) film on electrode surfaces in an organic solution, such as acetonitrile. The electrochemistry of the metallofullerene film is quite different from that of the dissolved Dy@C_{82}(I). Its reduction behavior is similar to that of the empty fullerene film,[27–29] that is, there are large splittings between the first two pairs of reduction and reoxidation waves. Significantly, however, a pair of reversible oxidation and rereduction waves has been observed, for which we put forward a plausible mechanism.

Results and Discussion

Cyclic voltammogram of the Dy@C_{82}(I) film on the electrode surface: Figure 1a displays a typical cyclic voltammogram (CV) of a Dy@C_{82}(I) film on a Pt electrode in acetonitrile containing tetrabutylammonium hexafluorophosphate ($TBAPF_6$) Several pronounced redox peaks are observed and highly reproducible, suggesting that the metallofullerenes on the electrode are electroactive in the organic solution. This is in contrast to the case of the La@C_{82} film in water,[30] where electron transfer is obstructed. As shown in Figure 1a, the first and second reduction waves appear at −0.8 V and −1.2 V (versus Ag/AgCl), respectively. These values are to be compared with the corresponding solution reduction waves at −0.2 V and −0.8 V (versus Ag/AgCl), respectively (see Figure 1b). When the potential scan is reversed toward the positive direction, large splittings between the reduction and reoxidation waves for the first and the second electron-transfer reactions are observed. This is very similar to the redox behavior of the C_{60} film,[27–29] although the wave splittings for the Dy@C_{82}(I) film are larger than for the C_{60} film (the first reduction wave: 1.2 V versus 0.5 V; the second reduction wave: 1.2 V versus 0.2 V). In contrast to the C_{60} film, however, an oxidation wave is observed during the subsequent positive scan and a cathodic wave associated with this oxidation wave appears upon further potential scan reversal to the negative direction. Interestingly, the potential separation between these anodic and cathodic peaks is 50 mV, which is in good agreement with the characteristic value of 59 mV for a reversible one-electron transfer. For the C_{60} film, in addition to the absence of a cathodic wave associated with its oxidation wave, the electroactivity of the film was found to diminish after cycling over the anodic wave.[27] However, the electroactivity of the Dy@C_{82}(I) film is maintained after many cycles of oxidation and rereduction waves (Figure 2). From the second scan cycle, the first reduction wave shifts positively to −0.4 V and remains in this position for the subsequent scans. The film is stable on Pt or ITO electrodes in the presence of $TBAPF_6$.

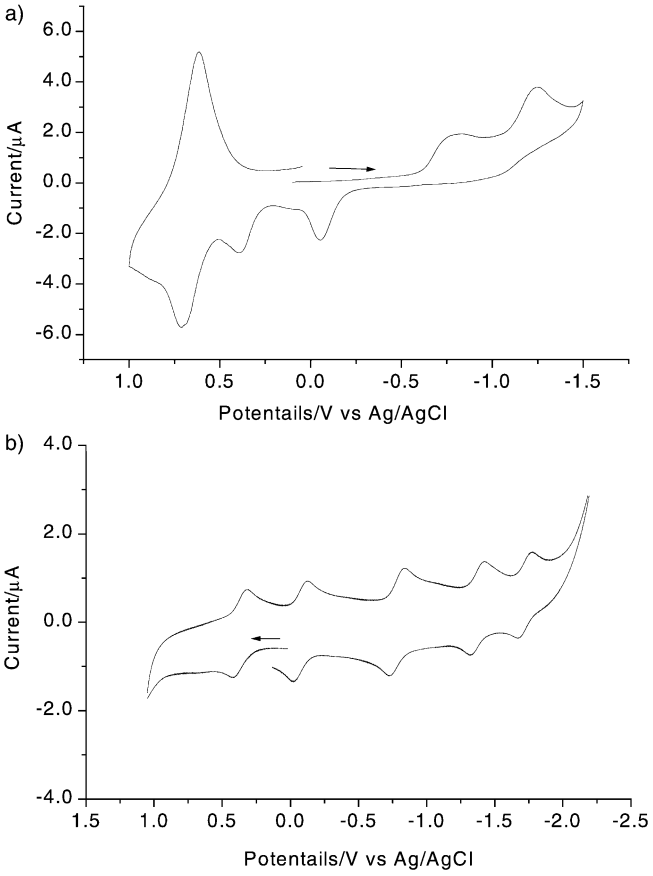

Figure 1. Cyclic voltammograms. a) A Dy@C_{82}(I) film on a Pt electrode (electrolyte: 0.1 M $TBAPF_6$ in MeCN; scan rate: 50 mV/s). b) A Dy@C_{82}(I) solution in toluene/MeCN (4:1, v) (electrolyte: 0.1 M $TBAPF_6$; scan rate: 50 mV s^{-1}).

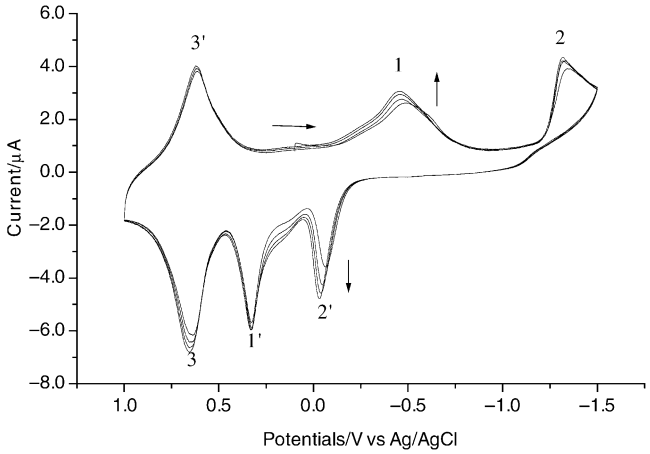

Figure 2. The second and subsequent cyclic voltammograms of a Dy@C_{82}(I) film on a Pt electrode (electrolyte: 0.1 M $TBAPF_6$ in MeCN; scan rate: 50 mV s^{-1}).

The first several scans over the first two reduction waves and the first oxidation wave cause only small changes in potential and small increases in peak current. In the subsequent cycles, both the potentials and currents of the redox waves are essentially unchanged even after 2 h of continuous scanning at 50 mV s^{-1}. However, the film starts to dissolve and the reduction waves become similar to those of the metallofullerene in solution when the potential is scanned beyond the third reduction wave. This is likely due to 1) the elevated negative potential which tends to desorb the negatively charged species, and 2) the increased solubility of the Dy@C_{82}^{n-}(I) species in the polar solvent acetonitrile as *n* increases.[29]

Characterization of the redox waves: *Cyclic voltammograms*: To examine the nature of the redox waves of the metallofullerene films in more detail, potential scans were carried out by setting starting and reversal potentials at different positions and in different directions. When the negative scan reversal is set at −1.1 V, that is, before the second reduction (see wave 2 in Figure 2) occurs, only one reoxidation wave at $E=+0.37$ V (versus Ag/AgCl) is observed (Figure 3a). If the negative potential scan reversal is extended negatively to −1.5 V, a cathodic wave 2 appears accompanied by an anodic wave 2′ (Figure 3b). This demonstrates unambiguously that the anodic wave 2′ and wave 1′ are associated with the cathodic wave 2 and wave 1, respectively.

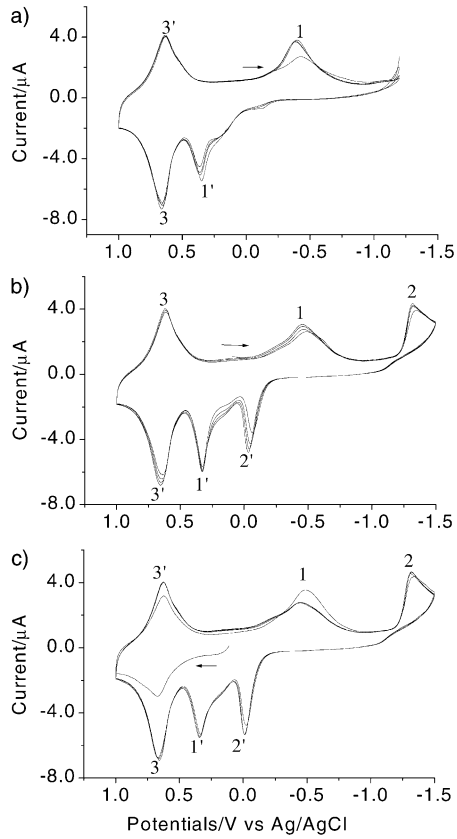

Figure 3. Cyclic voltammograms of a Dy@C_{82}(I) film on a Pt electrode with different starting and reversal points of potential scan (electrolyte: 0.1 M $TBAPF_6$ in MeCN; scan rate: 50 mV s^{-1}). a) Started in the negative scan direction with positive reversal at −1.1 V. b) Started in the negative scan direction with positive reversal at −1.5 V. c) Started at 0.10 V in the positive scan direction with negative reversal at 1.0 V.

On the other hand, if the potential scan is started at 0.1 V in the positive direction, only an anodic wave 3′ and a cathodic wave 3 are observed between 0.1 and 1.0 V (Figure 3c). In the subsequent potential scan cycles, the redox couples wave 1/wave 1′ and wave 2/wave 2′ show up again, suggesting that the wave 3′ is rereduction of the wave 3.

UV/Vis-NIR spectra: Akasaka et al. have shown that the electrogenerated La@C_{82}^- and La@C_{82}^+ are very stable in solution due to their closed electronic shell structures.[16,35] Here the electrogenerated metallofullerene monoanion and monocation are also quite stable in the films, and this has allowed us to further confirm the nature of wave 1 and wave 3 by spectroscopy. For the sake of comparison, we first present the solution phase UV/Vis-NIR absorption spectra of Dy@C_{82}(I), Dy@C_{82}(I)(−), and Dy@C_{82}(I)(+) in Figure 4a. As reported previously,[36] Dy@C_{82}(I) shows characteristic absorption bands at 640, 937, and 1400 nm. For Dy@

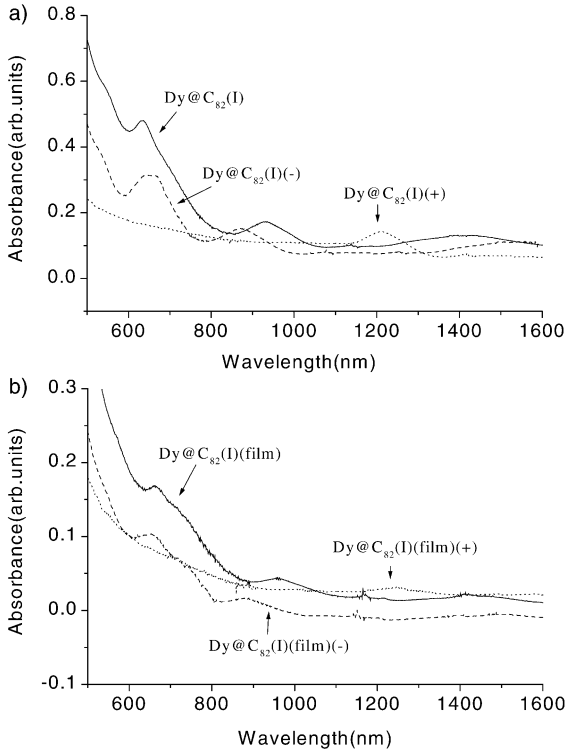

Figure 4. UV/Vis-NIR absorption spectra of Dy@C_{82}(I), Dy@C_{82}(I)(−), and Dy@C_{82}(I)(+). a) Solution of 0.1 M $TBAPF_6$ in toluene/MeCN (4:1, v). b) Film on ITO. The Dy@C_{82}(I)(−) and Dy@C_{82}(I)(+)) films were obtained by holding the electrode potential, respectively, right after wave 1 and wave 2 for ~10 s.

C_{82}(I)(−), there are also three absorption peaks, which are at 650, 880, and ~1570 nm. However, only one obvious absorption peak appears at 1210 nm for Dy@C_{82}(I)(+). Overall, the spectral features of both the anion and the cation are similar to those of La@C_{82}(I)(−) and La@C_{82}(I)(+), respectively,[16] but with small shifts. As for the corresponding films, no spectra have been reported until now. Figure 4b shows the UV/Vis-NIR absorption spectra of the corresponding species in the film on ITO. Except for some small spectral shifts, the one-to-one correspondence between the film spectra and the solution spectra is evident. Dy@C_{82}(I)(film) shows three peaks at 695, 950, and 1410 nm. Dy@C_{82}(I)(−)(film) shows three peaks at 655, 875, and ~1520 nm. Dy@C_{82}(I)(+)(film) shows only one peak at 1230 nm. By and large, the absorption peaks of the metallofulerene films are red-shifted from the corresponding spectra in solution due perhaps to the inter-metallofullerene interaction and/or the interaction between the metallofullerenes and the substrate/counterions. The Dy@C_{82}(I)(−) film was obtained by holding the electrode potential right after

wave 1 for ~10 s to ensure the complete conversion of Dy@C_{82}(I) to Dy@C_{82}(I)(−). Moreover, the spectrum of this film is similar to that of Dy@C_{82}(I)(−) in solution. These together verify that wave1 is associated with the reduction of Dy@C_{82}(I)(film) to Dy@C_{82}(I)(−)(film). By the same token, it is ascertained that wave 3 results from the oxidation of Dy@C_{82}(I)(film) to Dy@C_{82}(I)(+)(film) through the spectral comparison.

The reversible oxidation-rereduction couple: The reversible oxidation of the Dy@C_{82}(I) film is noteworthy. As Figure 5a demonstrates, such a reversible behavior is brought about only after certain structural organizations of a fresh film after the reduction/reoxidation wave. When the potential scan is started at 0.1 V (versus Ag/AgCl) toward the positive direction on a fresh film, the first oxidation wave and its corresponding rereduction wave appear at +0.90 V and +0.65 V (versus Ag/AgCl), respectively. The splitting between the initial two waves is as large as 0.25 V. However, in the second potential scan cycle, after the two pairs of the reduction/reoxidation waves are scanned through, the first oxidation wave is shifted negatively to +0.70 V, while its rereduction wave remains at +0.65 V. The resultant splitting of 50 mV is characteristic of a reversible redox couple. When the potential cycling is restricted to the range between −0.2 V and +0.9 V, that is, no reduction waves are involved, the oxidation and rereduction waves, although keeping their original positions, start to shrink continuously in the current amplitude as shown in Figure 5b. However, as the scanning potential range is extended to the first two reduction waves again, the oxidation/rereduction waves are recovered and the currents for the first oxidation wave and the rereduction wave remain constant after a few cycles (see Figure 5c). From these results, it is clear that a peculiar structure of the Dy@C_{82}(I) film after reoxidation of the reduced film is somehow responsible for the reversible oxidation of the film. Such a structurally reorganized neutral Dy@C_{82}(I) film is oxidized and rereduced on the electrode accompanied by the incorporation of PF_6^- ions into the film on the positive sweep and the expulsion of the same ions on the subsequent negative sweep in a reversible fashion, giving rise to a very small splitting value between the oxidation and rereduction waves. The proposed mechanism for the electrode processes is illustrated in Scheme 1. Similar to what was posited for C_{60} films,[27] we also attribute the large splittings between the first two pairs of the reduction/reoxidation waves of the Dy@C_{82}(I) film to the attendant structural reorganization of the film due to the accommodation of the bulky TBA^+ ions for charge balance. Note that the subscripts O, A, and B represent three different structural forms of the Dy@C_{82}(I) film: O denotes the original sample, B is a structurally modified form, and

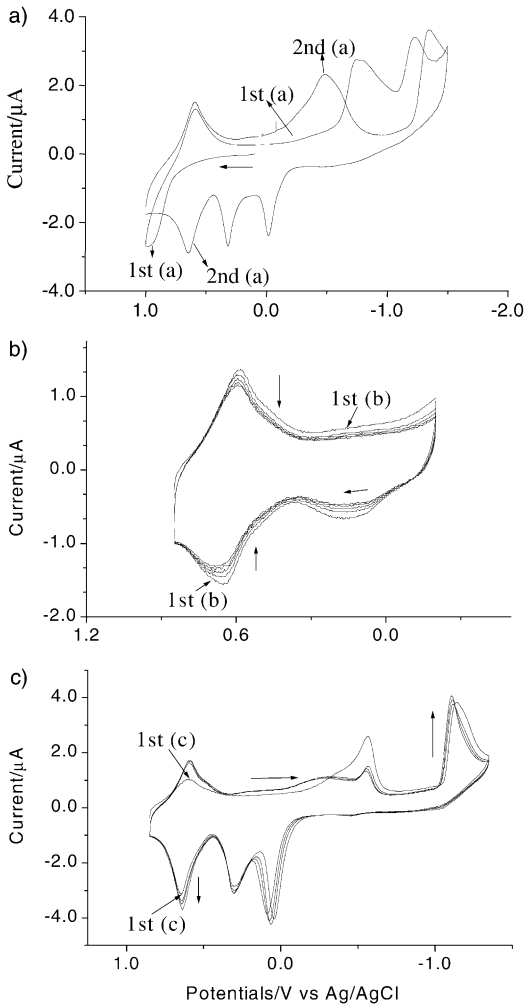

Figure 5. Cyclic voltammograms of a Dy@C_{82}(I) film on a Pt electrode with different starting points and potential scan range (electrolyte: 0.1 M $TBAPF_6$ in MeCN; scan rate: 50 mV s^{-1}). a) Two potential scan cycles between −1.5 V and 1.0 V started in the positive scan direction with a freshly cast film. b) Continuation of a) but the potential scan range has been narrowed down to between −0.2 V and 0.9 V. c) Continuation of b) but the potential scan range has been extended to between −1.5 V and 0.9 V.

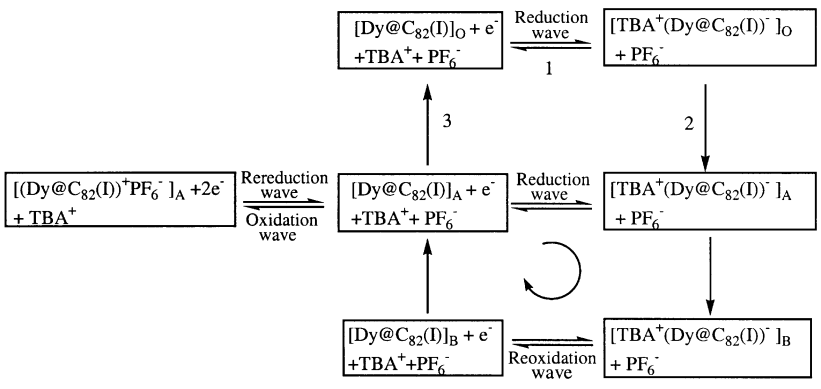

Scheme 1.

A is somewhere between O and A. More specifically, as $[Dy@C_{82}(I)(film)]_O$ is reduced to $[Dy@C_{82}(I)^-(film)]_O$, TBA^+ diffuses towards it to form $[TBA^+Dy@C_{82}(I)^-]_O$ (path 1). Because of the large size of TBA^+, its intercalation requires a structural reorganization of the metallofullerene film to an intermediate structure $[TBA^+Dy@C_{82}(I)^-]_A$ (path 2), and all the way to the stable intercalation structure $[TBA^+Dy@C_{82}(I)^-]_B$. Once this is completed, the potential cycling will follow the path indicated by the curved arrow as well as that of the oxidation/rereduction waves. This explains the large negative shift of the wave1 from the first to the subsequent scan cycles (see Figure 1a and Figure 2), and the large splittings of the reduction/reoxidation waves. The reorganized structure B is believed to be more open and accessible to TBA^+ so that the stable, charge-balanced ion pairs can be formed. After the reoxidation, the system enters an intermediate structure A, which accompanies the expulsion of TBA^+. Although somewhat relaxed from B, A is probably still quite open. Because PF_6^- is much smaller than TBA^+, it can easily get into and out of the intermediate structure A. In this case, the fast transport of the counterions is perhaps assisted by solvent molecules trapped in the pores of the film. As such, no structural reorganization is needed after the oxidation/rereduction of the film, hence a small splitting of the pair is obtained. In addition, the cycling indicated by the curved arrow is necessary for the reversible oxidation/rereduction because otherwise A may change slowly to O following the path 3 (Scheme 1). The symmetric shape, with $I_{pa}/I_{pc}=1.0$, of the oxidation and rereduction waves is typical of reversible electrode processes. The peak current I_p versus the scan rate v is plotted in Figure 6. Clearly, I_p is proportional to v for $v < 100\,mV\,s^{-1}$, indicating that the redox processes are confined on the electrode surface.[37] However, when the scan rate v is increased beyond $100\,mV\,s^{-1}$, both I_{pa} and I_{pc} deviate from the straight line; the increase of the peak current I_p becomes slower than that at the scan rate $v<100\,mV\,s^{-1}$. This suggests that kinetic factors of electron transfer begin to play important role at higher scan rates. Structural information of the metallofullerene films has also been obtained from SEM images. Figure 7 displays the SEM images of a $Dy@C_{82}(I)$ film on a Pt electrode before and after different electrochemical potential scans. The freshly coated film consists of small metallofullerene grains (<100 nm) with a uniform distribution (Figure 7a). Such a grain structure may be amenable to structural reorganization and to intercalation by foreign molecules. After electrochemical treatments, the $Dy@C_{82}(I)$ grain sizes on the electrode increase dramatically to the submicron and micron scales (Figure 7b and Figure 7c). This is consistent with what was reported for the C_{60} film,[38] and confirms the structural reorganization of the metallofullerene films. Although the details need further investigation, one may speculate that the structural reorganization involve the release of the solvent molecules trapped during evaporation and solvent-induced migration of the molecular species in the film. This would result in more open structures and consequently larger grain sizes as observed, which are then more accessible to the counter ions. The film images are rel-

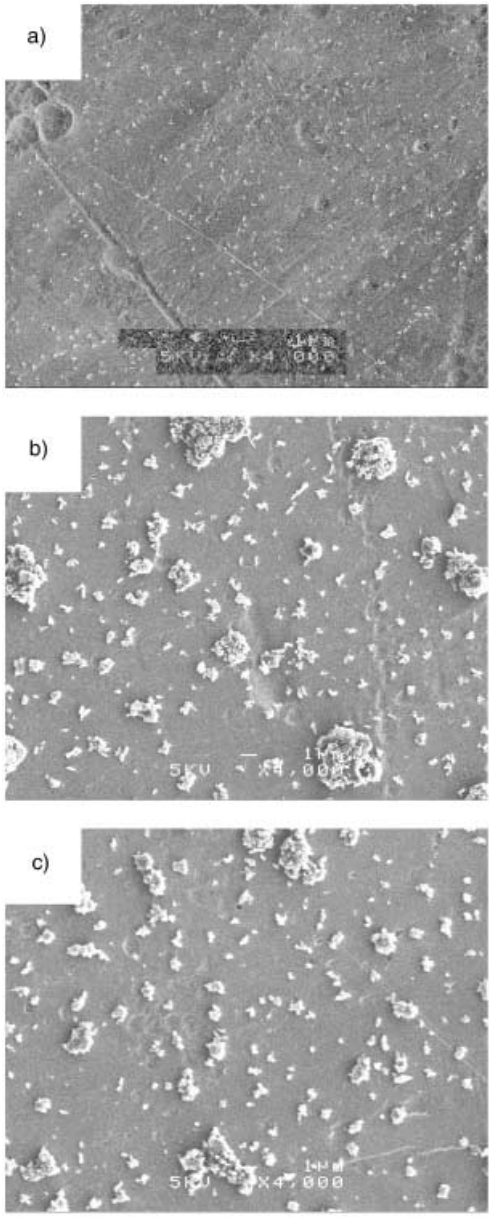

Figure 7. SEM images of $Dy@C_{82}(I)$ films. a) Freshly cast film. b) The film after the execution of the first two reduction and reoxidation waves. c) The film after completing the first oxidation and rereduction waves.

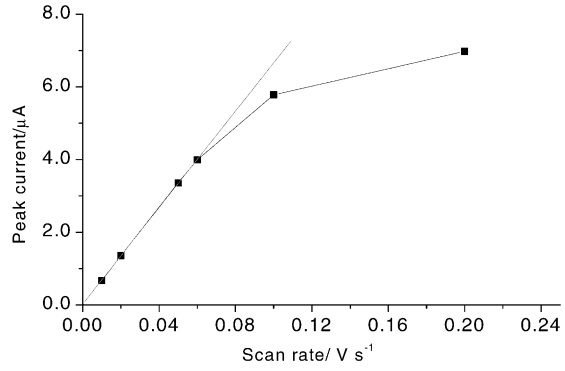

Figure 6. Relationship between the anodic peak current I_p and the scan rate for the first oxidation wave.

atively insensitive to the detailed procedures of the electrochemical treatment. For instance, the two films in Figure 7b and Figure 7c are very similar in morphology; one has experienced the first two reduction and reoxidation waves while the other has been subjected to only the first oxidation and rereduction waves.

Effects of the nature and sizes of the supporting electrolytes: Further evidence in support of the proposed mechanism has been gleaned from the influence of different supporting electrolytes on the electrochemical behavior of the metallofullerene film. For $Dy@C_{82}(I)/KPF_6$, the reduction/reoxidation behavior is similar to that of C_{60} under the same conditions with a small peak splitting (Figure 8a).[29] The splittings of the reduction/reoxidation waves for $Dy@C_{82}(I)/KPF_6$ (0.55 V for the first reduction and 0.073 V the second) are much smaller than in the $Dy@C_{82}(I)/TBAPF_6$ system (1.2 V for both the first and the second reductions). However, the oxidation wave of the film is not detected

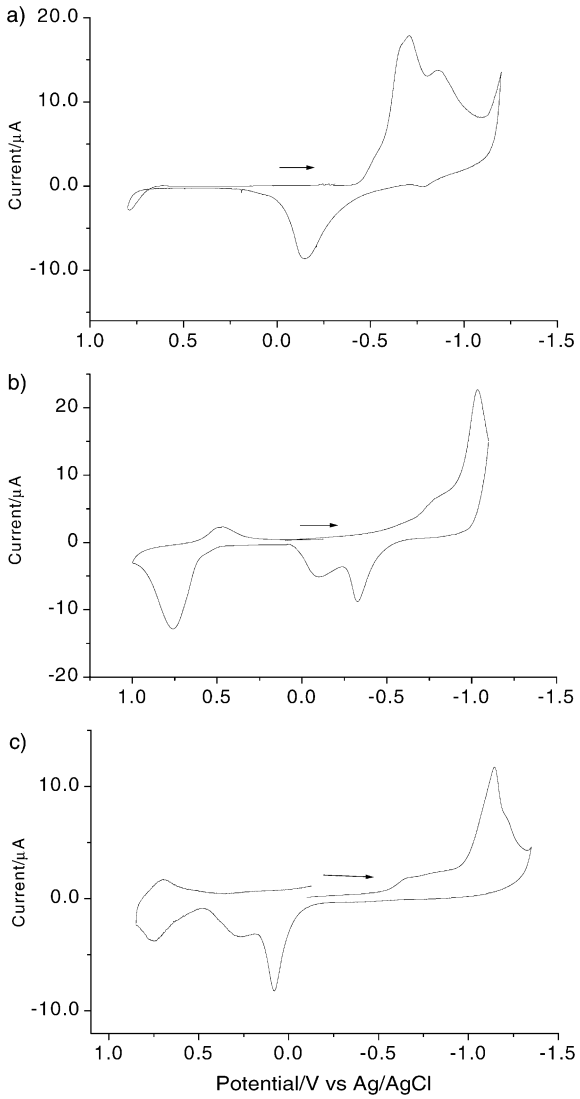

Figure 8. Cyclic voltammograms of a $Dy@C_{82}(I)$ film on a Pt electrode with different electrolytes in MeCN (scan rate: 50 mV s^{-1}). a) 0.1 M KPF_6. b) 0.1 M $LiClO_4$. c) 0.1 M $TBABF_4$.

even when the potential scan is extended positively to +1.3 V. Continuing the CV sweep for five or fewer cycles, the reduction waves disappear, signifying the vanishing electrochemical activity of the film. Analogous results have been obtained for $NaClO_4$. Taken together, it is the structure of the $Dy@C_{82}$ films that affects the film oxidation/rereduction. Certainly, smaller cations such as K^+ and Na^+ diffuse more rapidly and their intercalation into the metallofullerene films requires less extensive structural reorganizations. This results in the smaller reduction/reoxidation splittings we measured. The poorer stability of these films indicates that the formation of the $TBA^+Dy@C_{82}(I)^-$ ion pair is more favorable than that of the $M^+Dy@C_{82}(I)^-$ ion pair (M = K, Na) in the films. Finally, the less extensive structural reorganizations induced by the incorporation and expulsion of the alkali metal ions are likely to be the reason for the absence of the reversible oxidation/rereduction, which requires fast migration of the anions PF_6^- and ClO_4^- in the films. For $Dy@C_{82}(I)/LiClO_4$, a pair of oxidation/rereduction waves with a splitting of 0.20 V is obtained Figure 8b, while the splittings of the first and the second reduction/reoxidation waves are 0.74 V and 0.63 V, respectively. These splitting values are larger than those of $Dy@C_{82}/K^+$(or Na^+) but smaller than that of the $Dy@C_{82}/TBA^+$ system. However, after 10 or fewer cycles, the electrochemical activity of the film also fades away. Again, the likely explanation invoked for the C_{60} film may be operative here.[29] Here the reduced film of $Dy@C_{82}(I)$ with the inclusion of Li^+ seems to be more stable than those with K^+ and Na^+ perhaps for the reason that Li^+ is more strongly solvated by the nitrile molecules and the solvated Li^+ forms a more favorable ion pair with $Dy@C_{82}(I)^-$ in the film. Still, this film, with a larger splitting and intensity asymmetry of the oxidation/rereduction waves, is less stable than that with TBA^+. Moreover, the oxidized film with ClO_4^- is possibly less stable than that with PF_6^- due, once again, to the relative stabilities of the ion pairs in the films. The redox behavior observed for $Dy@C_{82}(I)/TBABF_4$ (Figure 8c) is close to that of $Dy@C_{82}(I)/TBAPF_6$. However, there are still some differences for these two systems. First, the peak currents of the oxidation and rereduction waves of $Dy@C_{82}(I)/TBABF_4$ are smaller than those of the reduction and reoxidation waves in contrast to the case of $Dy@C_{82}(I)/TBAPF_6$. Furthermore, the electrochemical activity decreases more quickly than for the $Dy@C_{82}(I)/TBAPF_6$ system when subjected to repeated potential cycling. This indicates that in film form, the $Dy@C_{82}(I)^+/BF_4^-$ ion pair is less favorable than the $Dy@C_{82}(I)^+/BF_4^-$ ion pair. To sum up, it appears that the electrochemical activity of the $Dy@C_{82}(I)$ film depend on the diffusivity of the counter ions, the structural reorganizations of the films, and the stability of the ion pairs, which is consistent with the mechanism proposed above.

Conclusion

For the first time, we have studied the electrochemical properties of pure metallofullerene films cast from $Dy@C_{82}(I)$ solutions in acetonitrile. The metallofullerene films are

stable against repeated potential cycling. The reduction and reoxidation responses of these films are similar to those of the C_{60} films, that is, there are large splittings between the first two reduction and reoxidation waves. In sharp contrast, however, a reversible pair of oxidation and rereduction waves with a splitting only 50 mV are successfully obtained for the Dy@C_{82}(I) films. It is demonstrated that these reversible oxidation and rereduction waves necessitate the structural reorganizations of the Dy@C_{82}(I) films, which can be induced by the reduction/reoxidation waves of the metallofullerenes. We have also shown the influence of the diffusivity of the counterions and the ion-pair stability on the electrochemical activity of the metallofullerene films. These results are clearly important, for example, with respect to the possible development of surface-modified electrodes by copolymerization with conductive polymers, with a broad range of applications in chemical/biochemical sensory devices.

Experimental Section

Materials and chemicals: High-purity Dy@C_{82} (99.5% as estimated with mass spectrometry) was prepared in our laboratory by a combination of the standard DC arc-discharge method and the isolation method described previously.[31–34] The raw soot from the arc-discharge was subjected to Soxlet extraction by using *N,N*-dimethylformamide (DMF) as the solvent, followed by HPLC separation using a 5PYE column with toluene as the mobile phase. Two isomers, Dy@C_{82}-I and Dy@C_{82}-II were readily separated by further separation using the same column. The identity and purity of the sample was verified by methane DCI negative ion mass spectrometry.

Acetonitrile (Labscan Asia Co., Ltd) of a high-performance liquid chromatography (HPLC) grade was used as received. Electrochemical-grade tetra-*n*-butylammonium hexafluorophosphate ($TBAPF_6$), and tetra-*n*-butylammonium tetrafluoroborate ($TBABF_4$), and potassium hexafluorophosphate (KPF_6) from Aldrich Chemical Co., lithium perchlorate ($LiClO_4$), and sodium perchlorate ($NaClO_4$) from Acros Organics Co. were dried in vacuum at 60 °C overnight before use.

Equipment and measurements: Cyclic voltammetry experiments were performed by using model 600 Electrochemical Analyzer from CH instruments Inc. USA, in a conventional three-electrode electrochemical cell at ambient temperature. A Pt wire electrode served as the auxiliary electrode, a Ag/AgCl electrode was used as the reference. All electrochemical experiments were performed in a high-purity N_2 atmosphere at ambient temperature (22 ± 1 °C). Scanning electron microscope (SEM) images were obtained with a field emission microscope (FSEM, JEOL JSM-6300F, Peabody, MA).

Dy@C_{82}(I) films were prepared as follows by drop coating of a 1.0 μL solution of Dy@C_{82}(I) in toluene (6.07×10^{-2} mol mL^{-1}) on a Pt disk, a Pt plate or an ITO electrode. This was followed by drying in a vacuum at ambient temperature for a period of 4 h. Bulk controlled-potential electrolysis was performed in a conventional H-type cell with a model 600 Electrochemical Analyzer from CH instruments Inc. USA. The working and auxiliary electrode compartments of the cell were separated with a sintered glass frit. Both the working and the auxiliary electrodes were made of platinum gauze. The anions and cations of Dy@C_{82}(I) (Dy@C_{82}(I)(−) and Dy@C_{82}(I)(+)) were obtained in the toluene/acetonitrile (4:1 by volume) solution containing 0.1 M $TBAPF_6$ by setting the applied potentials ~100 mV more negative or more positive than $E_{1/2}$ for the redox couples of Dy@C_{82}(I)/Dy@C_{82}^-(I) and Dy@C_{82}^+(I)/Dy@C_{82}(I), respectively. The extent of electrolysis for a given amount of Dy@C_{82}(I) in the solution was monitored by CV peak of Dy@C_{82}(I)(−) to Dy@C_{82}(I) (or Dy@C_{82}(I)(+) to Dy@C_{82}(I)): the electrolysis was continued until the CV peak stopped increasing. The time needed for a complete electrolysis of the solution was determined to be 10 min. The electrogenerated Dy@C_{82}(I)(−) and Dy@C_{82}(I)(+) were then transferred from the bulk cell to a quartz cuvette in a N_2 atmosphere. UV/Vis-NIR measurements were carried out with Perkin-Elmer LAMBDA 900 UV/Vis-NIR spectrometer under a N_2 atmosphere. For the film electrode, the same procedure was performed with the film on ITO (indium tin oxide) electrodes except that pure acetonitrile was used as the solvent. The electrolysis time for the full conversion of Dy@C_{82}(I)(film) to Dy@C_{82}(I)(−)(film) or Dy@C_{82}(I)(+)(film) was estimated to be 10 s.

Acknowledgement

This work was supported by an RGC grant administered by the UGC of Hong Kong. We thank MCPF of HKUST for assistance in sample characterization.

[1] S. Nagase, K. Kobayashi, T. Akasaka, T. Wakahara, in *Fullerenes: Chemistry, Physics and Technology*, (Eds.: K. M. Kadish, R. S. Ruoff), Wiley, New York, **2000**, p. 395.
[2] H. Shinahara, H. Sato, M. Ohkohchi, Y. Ando, T. Kodama, T. Shida, T. Kato, K. Saito, *Nature* **1992**, *357*, 52.
[3] E. Dietel, A. Hirsch, B. Pietzak, M. Waiblinger, K. Lips, A. Weidinger, A. Gruss, K. Dinse, *J. Am. Chem. Soc.* **1999**, *121*, 2432.
[4] B. Cao, M. Hasegawa, K. Okada, T. Tomiyama, T. Okazaki, K. Suenaga, H. Shinahara, *J. Am. Chem. Soc.* **2001**, *123*, 9679.
[5] Y. Chai, C. Guo, C. Jin, R. E. Haufler, L. P. Chibante, J. Fure, L. Wang, J. M. Alford, R. E. Smalley, *J. Phys. Chem.* **1991**, *95*, 7564.
[6] T. Akasaka, S. Nagase, K. Kobayashi, M. Walchli, K. Yamamoto, H. Funasaka, M. Kako, T. Hoshito, T. Erata, *Angew. Chem.* **1997**, *109*, 1716; *Angew. Chem. Int. Ed. Engl.* **1997**, *36*, 1643.
[7] W. Sato, K. Sueki, K. Kikuchi, K. Kobayashi, S. Suzuki, Y. Achiba, H. Nakahara, Y. Ohkuba, F. Ambe, K. Asai, *Phys. Rev. Lett.* **1998**, *80*, 133.
[8] T. Suzuki, Y. Maruyama, T. Kato, K. Kikuchi, Y. Achiba, *J. Am. Chem. Soc.* **1993**, *115*, 11006.
[9] Q. Li, F. Wudl, C. Thilgen, R. L. Whetten, F. Diederich, *J. Am. Chem. Soc.* **1992**, *114*, 3994.
[10] D. Dubois, K. M. Kadish, S. Flanagan, L. Wilson, *J. Am. Chem. Soc.* **1991**, *113*, 7773.
[11] M. S. Meier, T. F. Guarr, J. P. Selegue, V. K. Vance, *J. Chem. Soc. Chem. Commun.* **1993**, 63.
[12] T. Suzuki, K. Kikuchi, F. Oguri, Y. Nakao, S. Shinzo, Y. Achiba, K. Yamamoto, H. Funasaka, T. Takahashi, *Tetrahedron* **1996**, *52*, 4973.
[13] H. Shinohara, *Rep. Prog. Phys.* **2000**, 63, 843; S. H. Yang, *Trends in Chemical Physics* **2001**, 9, 31.
[14] M. R. Anderson, H. C. Dorn, S. A. Stevenson, *Carbon* **2000**, *38*, 1663.
[15] W. L. Wang, J. Q. Ding, S. H. Yang, X.-Y. Li, in *Recent Advances in Chemistry and Physics of Fullerenes and Related Materials, vol. 4*, (Eds.: K. M. Kadish, R. S. Ruoff), Electrochemical Society, Pennington, **1997**, p. 417.
[16] T. Akasaka, T. Wakahara, S. Nagase, K. Kobayashi, M. Waelchli, K. Yamamoto, M. Kondo, S. Shirakura, S. Okubo, Y. Maeda, T. Kato, X. Gao, E. V. Caemelbecke, K. M. Kadish, *J. Am. Chem. Soc.* **2000**, *122*, 9316.
[17] K. Kikuchi, S. Suzuki, Y. Nakao, H. Nakahara, T. Wakabayashi, H. Shiromaru, K. Saito, I. Ikemoto. Y. Achiba, *Chem. Phys. Lett.* **1993**, *216*, 67.
[18] K. Yamamoto, H. Funasaka, T. Takahashi, T. Akasaka, *J. Phys. Chem.* **1994**, *98*, 2008.
[19] K. Yamamoto, H. Funasaka, T. Takahashi, T. Akasaka, *J. Phys. Chem.* **1994**, *98*, 12831.
[20] T. Wakabayashi, S. Okubo, M. Kondo, Y. Maeda, T. Akasaka, M. Waelchli, M. Kako, K. Kobayashi, S. Nagase, T. Kato, K. Yamamoto, X. Gao, E. Caemelbecke, K. M. Kadish, *Chem. Phys. Lett.* **2002**, *360*, 235.
[21] T. Akasaka, S. Okubo, M. Kondo, Y. Maeda, T. Wakahara, T. Kato, T. Suzuki, K. Yamamoto, K. Kobayashi, S. Nagase, *Chem. Phys. Lett.* **2000**, *319*, 153.

[22] R. C. Haddon, *Acc. Chem. Res.* **1992**, *25*, 127.
[23] S. Chakravarty, M. P. Gelfand, S. Kivelson, *Science* **1991**, *254*, 970.
[24] P. W. Stephens, D. Cox, J. W. Lauher, L. Mihaly, J. B. Wiley, P. Allemand, A. Holczer, Q. Li, J. D. Thompson, F. Wudl, *Nature* **1992**, *355*, 331.
[25] Q. Gong, Y. Sun, Z. Xin, Y. Zou, Z. Gu, X. Zhou, D. Qiang, *J. Appl. Phys.* **1992**, 71, 3025.
[26] B. Miller, J. M. Rosamilia, G. Dabbagh, R, Tycko, R. Haddon, A. J. Muller, W. Wilson, D. W. Murphy, A. F. Hebard, *J. Am. Chem. Soc.* **1991**, *113*, 6291.
[27] J. Christophe, A. J. Bard, F. Wudl, *J. Am. Chem. Soc.* **1991**, *113*, 5456.
[28] W. Kob, D. Dubis, K. Wloszimier, M. T. Thomas, K. M. Kadish, *J. Phys. Chem.* **1993**, *97*, 6871.
[29] J. Chlistunoff, D. Cliffel, A. J. Bard, *Thin Solid Films* **1995**, 257, 166.
[30] N. Nakashima, M. Sakai, H. Murakami, T. Sagara, T. Wakahara, T. Akasaka, *J. Phys. Chem.* B **2002**, 106, 3523.
[31] Y. F. Lian, S. F. Yang, S. H. Yang, *J. Phys. Chem.* B **2002**, 106, 3112.
[32] J. Q. Ding, S. H. Yang, *Chem. Mater.* **1996**, *8*, 2824.
[33] J. Q. Ding, L. T. Weng, S. H. Yang, *J. Phys. Chem.* **1996**, *100*, 11120.
[34] H. J. Huang, S. H. Yang, *J. Phys. Chem.* B **1998**, 102, 10196.
[35] T. Akasaka, T. Wakahara, S. Nagase, K. Kobayashi, M. Waelchli, K. Yamamoto, M. Kondo, S. Shirakura, Y. Maeda, T. Kato, M. Kako, Y. Nakadara, X. Gao, E. Caemelbecke, K. M. Kadish, *J. Phys. Chem.* B **2001**, 105, 2971.
[36] N. Tagmatarchis, H. Shinohara, *Chem. Mater.* **2000**, *12*, 3222.
[37] A. J. Bard, L. R. Faulkner, *Electrochemical Methods: Fundamentals and Applications*, New York, John Wiley, c **2001**.
[38] C. Jehoulet, Y. S. Obeng, Y. Kim, F. Zhou, A. J. Bard, *J. Am. Chem. Soc.* **1992**, *114*, 4237.

Received: February 25, 2003
Revised: May 16, 2003 [F4882]

